31st Congress of the International Council of the Aeronautical Sciences

Belo Horizonte, Brazil; September 09-14, 2018

A SIMULATION MODELING STUDY FOR FREE ROUTING AIRSPACE IN JAPAN

Kota Kageyama* , **Yoichi Nakamura***
***Electronic Navigation Research Institute**

Keywords: *Air Traffic Management, Simulation, Free Routing, Airspace Sectorization*

Abstract

The free routing airspace in which users are able to plan a user preferred route (UPR) based on user-defined segments is intended to be implemented in radar air traffic control (ATC) airspace. According to this implementation plan, airspace sectrization will play an important role. For the purpose, consideration of an air traffic control officer (ATCO)' s workload is indispensable.

This paper presents an exemplary simulation study of this workload. A simulation model is built to estimate the impact of UPRs upon the workload in a Japanese ATC sector. After a validation study, UPR routes are applied to the model. The workload is estimated and the impact of UPR in the sector is discussed.

1 Introduction

In Japan, plans to implement free routing airspace (FRA) in radar air traffic control (ATC) airspace are underway. Because the airspace handles a large number of flights, consideration on the sector capacity is indispensable for the implementation plan.

The capacity is determined based on the workload measured by the ATC communication volume in the actual operation and in human-in-the-loop (HITL) simulation[1][2].

Constant workload values are applicable to the current fixed route structure. On the other hand, for the user preferred route (UPR) operations in radar ATC airspace, workload needs to be re-estimated in accordance with the route structure. Fast-time simulation is a useful technique for estimating workload in an efficient manner.

A fast-time simulation model is built to estimate the air traffic control officer (ATCO)s' workload. For the purpose of this estimation, the simulation events are converted into the corresponding communication issuances.

The simulation model should capture the traffic flow and ATC behavior[3]. This is validated by analyzing the transit-time, climb-profiles and the communication issuance frequency. Finally, a day with very windy condition day is chosen as an example and fuel-optimal routes are applied to the model. The fuel-optimal routes are regarded as a representative example of UPR. From the simulation results, the ATCOs' workload during UPR operations is estimated and discussed.

2 The Sector Capacity

To expedite safe and efficient flow, the capacity for each sector is determined, and this quantity expresses the maximum number of flights that can be served in the sector during a given period of time. The capacity is determined based on ATCOs' workload. For Japanese ATC operations, workload is measured based on the modified Messerschmitt Bölkow Blohm (MMBB) method, which considers ATC communication volume. The required times for decision making and other background tasks including surveillance are added to this volume.

This method classifies tasks into the following nine items, *Control transfer, Approach clearance, Altitude change, Holding, Traffic informa-*

tion, Route change, Heading, Direct and *Speed*.

The model converts the tasks into distinct segments of the timeline[4]. The method expresses the workload metric G as

$$G = \sum_{j=1}^{9} \tau_j \cdot \lambda_j \tag{1}$$

Here, τ_j is the time required to complete task j; λ_j is the issuance frequency of task i. For each sector, the communication frequency and duration during the actual operations/HITL simulation are analyzed to define the values of τ_j and λ_j. Because decision-making and other background tasks are included, the value of τ is greater than the observed duration of transmission. Subject matter experts (SMEs) decide this value.

Let us denote the averaged transit-time as F. The required workload per unit time is described as

$$Q = G/F \tag{2}$$

The transit-time within a time-bin (e.g. 30 minutes) for flight i is denoted by t_i. The workload in this time-bin is estimated as

$$S = \sum_i Q \cdot t_i \tag{3}$$

The upper-limit of the workload in a bin is separately defined. When S exceeds the upper-limit, the traffic volume is arranged by means of intervening departure-time or rerouting. The ground delay programs (GDPs) are the primary technique for making this arrangement. Although two ATCOs, the radar (tactical) controller and the coordinator (planning controller), are essentially assigned to each sector, the method particularly covers only the radar controller.

3 The Simulation Model

3.1 The Modeled Sector

One Japanese sector (T26) is modeled, since this sector chiefly handles the flights in the cruise phase; free routing airspace (FRA) is usually assumed during this phase[5]. Figure 1 shows the traffic flows and sector boundary of the modeled sector.

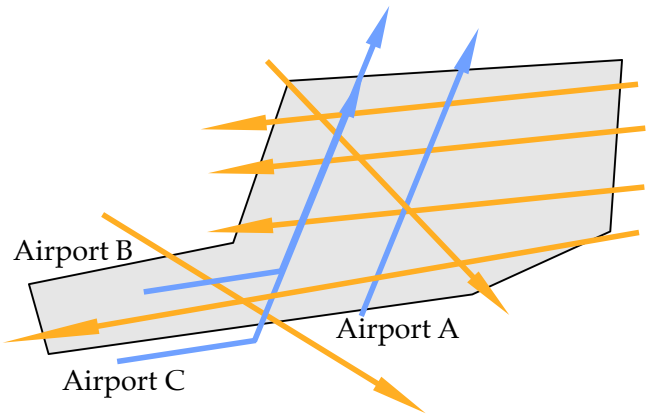

Fig. 1 The traffic flows and sector boundary

In the vicinity of the sector, three airports (*Airports A, B* and *C*) exist. The blue arrows represent the flow of the departure from the airports: the orange arrows represent the other flows in the sector. The essential task in this sector is to assure separation between the departure and other flows.

The model employs AirTOp V2.3 fast-time simulation software, which enables detailed modeling of the ATC procedure[6]. BADA 3 is used as the aircraft performance data [7].

3.2 The Workload Estimation

Following the concept of the MMBB method, the ATCOs' workload is modeled. In Equation (1), the operational values are applied for τ and the model is used to estimate the frequency λ of the ATC communication items.

The ATC communication items can be divided into categories of **Routine** or **Irregular**. For instance, every time a flight enters or leaves the sector, *Control transfer* is required. This item is thus classified as **Routine**. The occurrence of the corresponding events (sector entry and sector exit) triggers the issuance of this item.

On the other hand, because the *Heading* item is issued only when required, it is classified as **Irregular**.

Other examples of conversions are as follows:

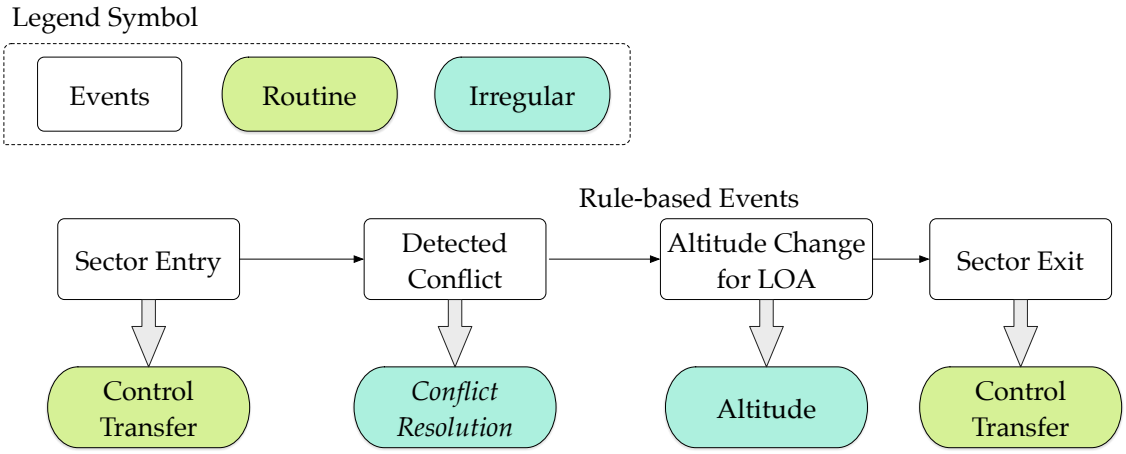

Fig. 2 The simulation-events conversion

- ***Altitude change*** ··· To comply with letter of agreement (LOA) constraints, the flights that leave the sector via the designated exit-waypoint are required to descend to the designated altitude. On the other hand, the flights from the adjacent airport are required to climb to the designated altitude. These items are regarded as **Irregular**. The rule-base function in the software reproduces the altitude change. The altitude may also be changed to assure separation between aircraft (conflict resolution). The modeling of the separation assurance maneuvers is discussed in the next subsection.

- ***H*eading**, ***D*irect** and ***Speed*** ··· The items of *Heading*, *Direct* and *Speed* are mainly issued for separation assurance (conflict resolution and LOA regulations). The frequency depends on the traffic situation. These items are classified as **Irregular** and the modeling of the conflict resolution is discussed in the next subsection. Since the instances were rarely observed in actual operation data, LOA regulations cases are also neglected. Items like **Heading** and **Direct** may be issued for other purposes, such as adverse weather avoidance. Assuming the frequency is minor, these cases are neglected.

Figure 2 shows examples of the post-processing for converting events into communications issuances.

3.3 The Conversion of Conflict Resolution

Conflict resolution serves to enforce both lateral and vertical radar separation minima. If separation minima are likely to be violated, ATCOs issue ATC instructions. The simulation software has the function of conflict detection. On the other hand, the software is not able to resolve conflicts in the same manner as ATCOs.

Since the purpose of this study is to estimate the workload, the model merely detects the violations of the minima and converts them into the ATC communications. For the purpose of conversion, the actual data are analyzed. Because the communication data are not available, the trajectories from the radar data are exploited to infer the issued items.

28 days' worth of the radar data are gathered and played back to pick up conflict resolution cases. The data are from the radar data processing system (RDP) in which the coordinates of actual trajectories are recorded at 10-seconds intervals.

1,543 conflict resolution cases were picked out of the radar data. The cases in which heading, altitude or speed changed for conflict resolution were extracted and the items were inferred.

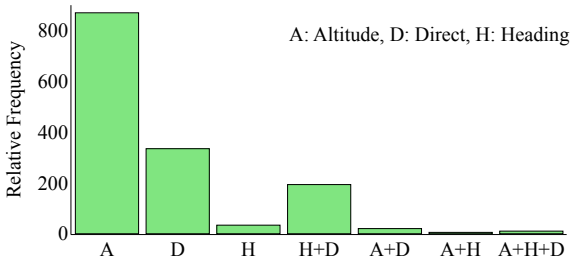

Fig. 3 Relative frequency of ATC issuance

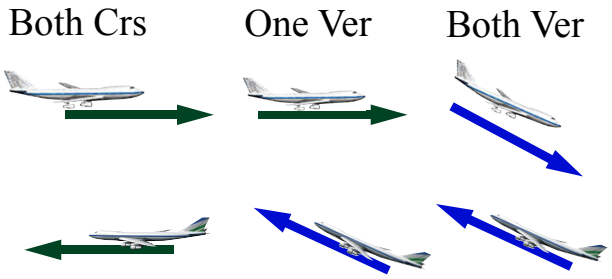

Fig. 4 Classification of vertical relationship

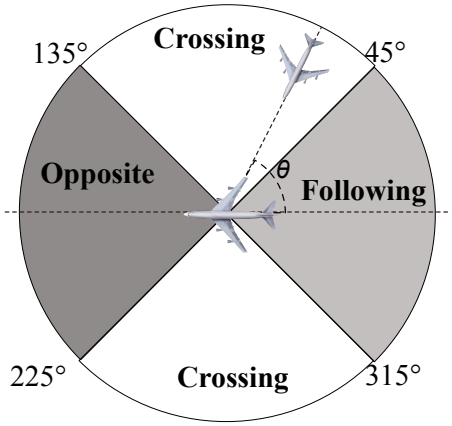

Fig. 5 Classification of flight angle

It is possible that minor speed changes may be neglected using this method.

Figure 3 shows relative frequency of the inferred items. The relative frequency of the item j can be regarded as the issuance probability p_j for a conflict resolution.

Denoting the duration of each item by κ_i, the expected communication duration can be computed as

$$C = \sum_{j=1} p_j \cdot \kappa_j \tag{4}$$

To obtain the workload C for a conflict resolution, the values of p and κ should be defined. Since the items are common, the corresponding λ_i in Equation (1) is used as κ_j. In the case that combined ATC instructions (e.g. "**Altitude+Direct**") are issued, κ is denoted as the sum of the λ values.

For detailed modeling, the detected conflict is classified into the cases based on the positional relationship between pairs of the flights. This relationship is known to influence to the ATCOs ' workload[3]. The vertical relationship is defined as **BothCrs**, **OneVer** and **BothVer** (Figure 4). At the same time, based on the flight-angle θ, the three cases (**Following**, **Crossing**, **Opposite**) are defined as shown in Figure 5. For each of the positional relationship cases, probability p is defined. Consequently, the workload C for conflict resolution is computed as in Table 1.

In addition to the current sector, this model covers conflicts in the next sector. In the actual operations, in case conflicts are predicted to occur in the next sector, ATC instructions can be issued to resolve conflicts in early stages. Taking this maneuver into a consideration, conflicts detected in the next sector increased the workload. For simplicity, **Direct** is assumed to be issued for the conflict in the next sector and corresponding value is added.

4 The Validation of the Model

4.1 The Transit-time

The scenario data define the initial states of the trajectories (i.e. positions and altitudes). The scenarios are put into the software to simulate

Table 1 Workload for conflict resolution (sec.)

	Following	Crossing	Opposite
BothCrs	26	37	24
OneVer	30	35	34
BothVer	33	35	36

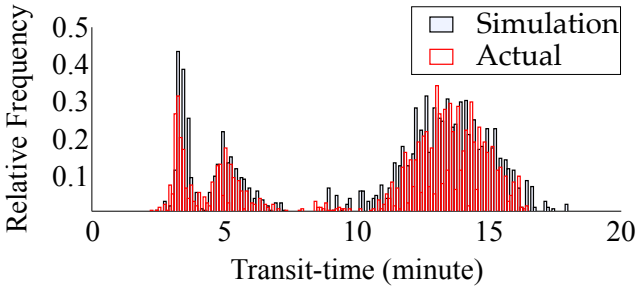

Fig. 6 Distribution of the transit-time

Table 2 Transit-time estimation error (minutes)

Category	Flights #	Ave.	S.D.
All	2,518	0.13	1.09
Over	2,124	0.09	1.10
Dep	394	0.30	1.00

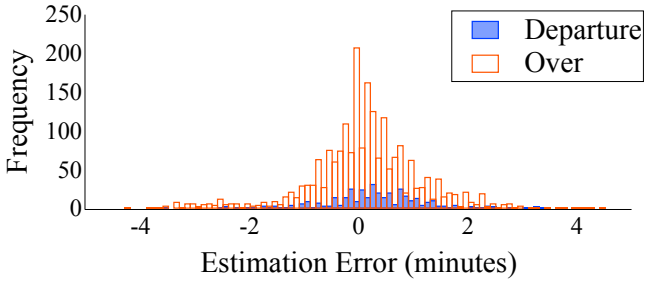

Fig. 7 Distribution of the estimation-error

the trajectories after the initial states. To obtain reliable results, the model should reproduce actual trajectories. Because they are used for the workload computation (Equation (2)), the transit-times in the model should be close to the actual values.

11 days' worth of trajectories from the radar data are gathered to validate the transit-time. The flight trajectories often deviate from the planned routes during the actual operation. Since it is difficult to measure this impact of the deviation, the flights that exactly followed the planned routes are extracted. Using wind-data for the corresponding times, the flights were modeled to validate the transit-time.

Figure 6 shows a comparison of the relative distribution of the transit-time. From the chart, the two distributions were observed to show similarity.

Because the characteristics are different, traffic flows in this sector are divided into two categories as follows. Departures from the adjacent airports (Airport A, B and C) are referred to as **Dep**; the other flights are referred to as **Over**.

Deducting the actual value from the estimated one, the estimation errors are computed. Table 2 shows the averages and the standard deviations of the error. **Over** accounted for a large portion of the flights. The ratios of the errors are 3% (**Over**), 9% (**Dep**). The averaged error of **Dep** is slightly larger than that of **Over**. Figure 7 shows the distribution of the error.

4.2 The Climb-profile

To study the increased average of the estimation error for **Dep** flights, their climb-profiles are analyzed. Figures 8 and 9 show examples of the actual climb-profiles for the aircraft type DHC8. In the figures, actual climb-profiles are compared with a simulation model. Figure 8 shows a steep climb-profile. Since the altitude of 15,000ft is the boundary between the modeled sector (T26) and the terminal areas of the airports, steep climb-profiles promoted early sector entry whereas gentle climb-profiles retarded this entry. The figures imply a variety of climbing maneuvers during actual operations. To improve the fidelity of the climb-profiles in the model, diversification of the climb maneuver should be modeled.

4.3 The Workload Estimation

For validation, the estimated communication volume is compared with the sampled observation data. These data were observed on different dates

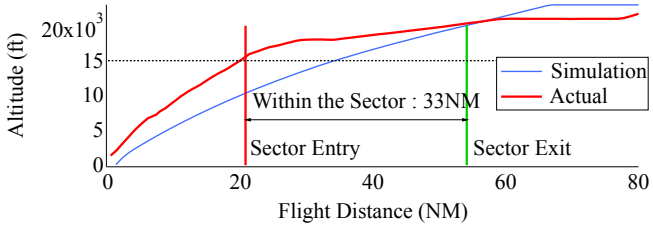

Fig. 8 climb-profile (Steep)

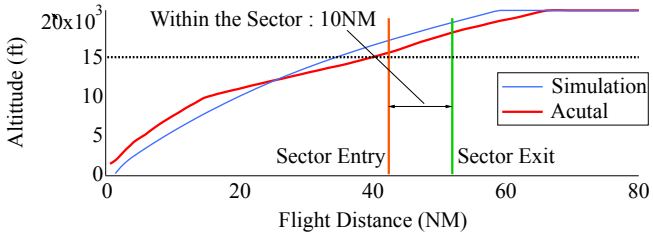

Fig. 9 climb-profile (Gentle)

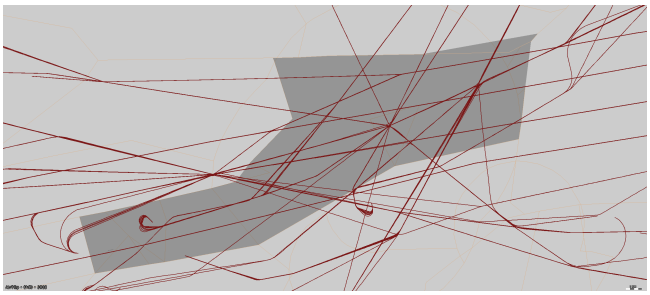

Fig. 10 Trajectoires (Baseline)

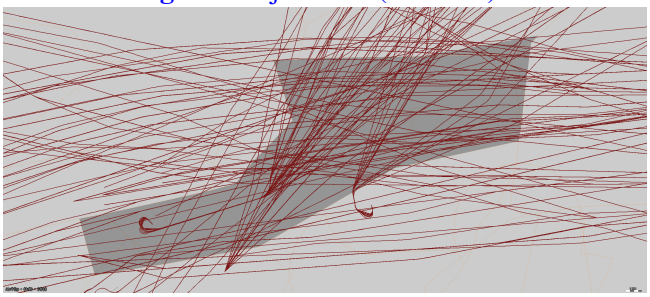

Fig. 11 Trajectories (UPR)

from the model.

For conflict resolutions and LOA regulations, **Irregular** items accounted for 6.8 seconds (the model) or 5.7 seconds (the observation data) of the workload. The estimate is 20% bigger than the observational data.

The average total of all items is 41.32 seconds (the model) and 40.2 seconds (the observation data). Good agreement was obtained with this model.

Since the recording dates differ, an exact comparison between the estimation results and the observed data is difficult. Still, the results of the comparison show that the model did not differ from the actual values.

5 The Modeling of the Free Routing

5.1 The Route Computation

A particularly windy condition day is chosen for consideration and optimal routes are computed based on the combination of origin and destination airports and aircraft types. This study assumes that the route that minimizes fuel consumption route is desirable for all users. Moreover, it is assumed that airspace users are able to plan the optimal routes between the two points corresponding to the starting- and ending-points.

The starting-points are basically defined as the end points of standard instrument departure (SID)s; the end-points are basically defined as the start points of standard instrument arrival (STAR)s. If the origin/destination airports are outside Japan, the gate fixes of the Japanese flight Information region (FIR) are used as the starting/ending points.

The fuel-optimal trajectories between two points are generated using the moving search space dynamic programming to minimize the evaluated fuel-burn function (fuel-burn)[8].

Based on the flight-plan data recorded on the corresponding day, the scenario data are prepared for the model. The flights that pass through the sector are assumed to be controlled in that sector. This model is referred to as a *UPR* model.

At the same time, the current fixed routes are also applied to the same scenario. This model is referred to as a *baseline* model.

5.2 Comparison of Trajectories

Figures 10 and 11 respectively show the trajectories from the *baseline* and *UPR* models. The

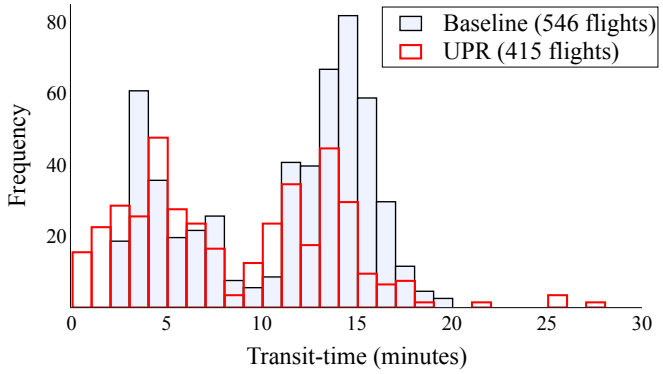

Fig. 12 Distribution of the Transit-time

UPR model decreased the number of the controlled flights from 546 to 415; alternatively, the route structure increased the volume in the other sectors.

In *baseline* model, the flights with the same origin and destination airport pair share the identical flight routes. On the other hand, in the *UPR* model, even though the airport pair is common, the optimal routes differ slightly depending on the aircraft types. The UPR trajectories thus show the scattering.

For airspace sectorization, some constraints exist. One such constraint is the minimum transit-time. The controlled flights must stay within a sector for a given minimum amount of time for coordination work to pay off and that conflict management to become possible[9].

Figure 12 shows the distribution of the transit-time from the models. From the chart, it was observed that the transit-times of some flights took small values (e.g. less than 2 minutes). To accommodate this constraint, the route or sectorization should be arranged.

5.3 The Workload Comparison

Workload is compared between the two models. As mentioned in 5.2, the UPR model showed a scattered trajectory. This change in the trajectory structure might affect the difficulty of the tasks. In the *baseline* model, since the number of interference points is limited, the conflict resolution strategy can be broken down into patterns; in the *UPR* model, because the interference points are scattered over a broad areas, the difficulty may be increased. On the other hand, because these trajectories are scattered, UPR provides more room for conflict resolution. That is, the difficulty of conflict resolution might be decreased in UPR.

Table 3 The Workload and Transit-time (minutes)

Model	Cat	W/L	Trans.	Q
baseline	Over	.64	11.1	.06
	Dep	1.24	9.9	.13
UPR	Over	.65	9.1	.07
	Dep	1.23	7.2	.17

On the assumption that the future ATM systems implement accurate conflict probe function to moderate the difficulty concerning the decision-making for conflict resolutions, constant values of κ (Equation (4)) in the *baseline* model are applied to the *UPR* model

Table 3 shows a comparison between the models for the averaged workload, transit-time and Q. From the table, the workload averages were observed to be almost equivalent. On the other hand, transit-time is decreased in the *UPR* model. Because of the decreased transit-time, UPR increased the value of Q by 22%(**Over**) and 39%(**Dep**), respectively.

Figure 13 compares the *baseline* and *UPR* rates for **Routine** items, LOA regulations and conflict resolution. It was observed that the difference in workload can mainly be attributed to LOA. The route structure change increased the number of **Dep** flights. Because LOA regulations were imposed on the flights, the workload for LOA increased.

It should be noted that the proportion of the detected conflicts was rather small compared to the total workload. Thus, the magnitude of the error for the conflict resolution did not much affect estimates for total workload.

The transitions of the workload over the time-bins are computed. Using Equation (3), the workload S for a 30 minute time-bin is computed.

Figures 14 and 15 show the computation re-

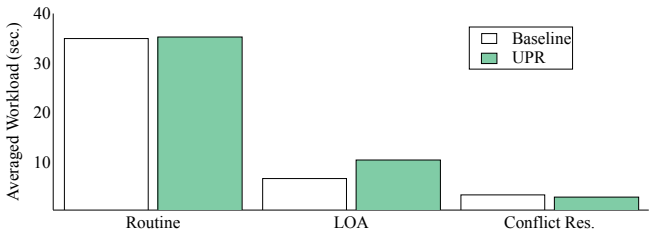

Fig. 13 Comparisons of workload times spent on the classifications of the items

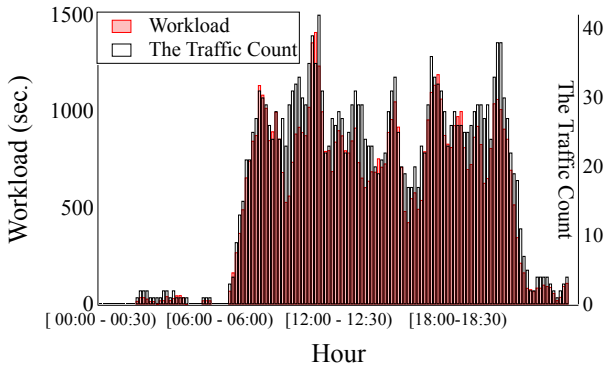

Fig. 14 The transition of the workload (Baseline)

sults. In the charts, the starting-time of the time-bin is advanced by 10 minutes. From the figures, it was confirmed that the change tendency of the workload was similar to that for the controlled flights in both models. The difference can be attributed to the proportions of the categories.

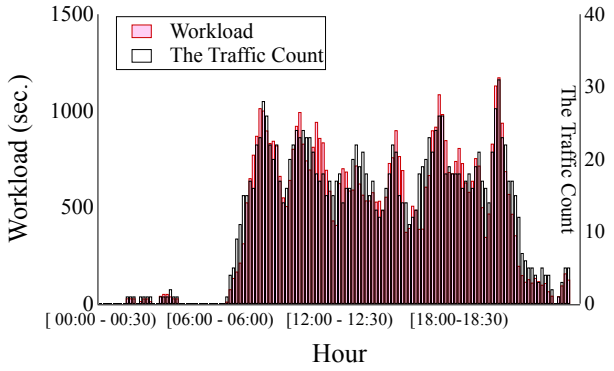

Fig. 15 The transition of the workload (UPR)

6 Conclusion

A fast-time simulation model was constructed for the Japanese ATC sector to estimate the ATCOs' workload. For the purpose of this estimation, the simulation events were converted into issuance of the ATC communications.

The transit-time was validated. Although the fidelity of **Dep** deteriorated due to the variability of the climb-profile, the model agreed with the actual data to a certain degree. The estimated workload demonstrated similarity to the values used in the operations.

One particularly windy condition day was chosen and the fuel-optimal routes were computed and applied to the model. The current sector boundary produces an unacceptably short transit-time. That is, sector boundary needs to be arranged differently.

For the ATCOs' workload, the following results were observed. In the modeled sector, the conflict resolution items affected the workload less than did **Routine** items (control transfer). This implied that, as long as a high-fidelity flight profile is provided in the simulation, the workload can be estimated by this methodology. However, the proportion of the items depends on the sector. If conflict resolution accounts for a large proportion of the workload, a more precise methodology should be studied.

At the same time, it should be emphasized that a future ATM function that mitigates the increased traffic complexity was assumed and that the impact of scattered trajectories for the workload was not considered in this study.

To accommodate UPR in the radar ATC space, prediction of the traffic flow as well as ATCOs' workload is indispensable. Fast-time simulation should be considered to be powerful means of the prediction.

Acknowledgements

The authors are grateful to JCAB (Japan Civil Aviation Bureau), the Ministry of Land, Infrastructure and Transport and Tourism, Japan for their cooperation in the acquisition of the actual

data.

Special thanks should be attributed to Dr. Yoshikazu Miyazawa for the computation of the fuel-optimal routes. Furthermore, the authors would like to thank Mr. Kazuo Akinaga for his assistance.

References

[1] Tofukuji N., "An Enroute ATC Simulation Experiment for Sector Capacity Estimation," *IEEE Trans. on Control Systems Technology*, Vol. 1, No. 3, 1993, pp. 138 – 143.

[2] Uelé, N. R. and Garcia J. M. C. "Relationship between Workload and Duration of ATC Voice Communication," *International Conference on Research in Air Transportation*, 2014.

[3] Volf P., Jakubův J. and Koranda L., "Validation of an Air-Traffic Controller Behavioral Model for Fast Time Simulation," *Integrated Communications, Navigation and Surveillance Conference (ICNS)*, 2014.

[4] Welch J. D., John W. Andrews and Martin B. D., "Macroscopic Workload Model for Estimating En Route Sector Capacity," *7th USA/Europe Air Traffic management R&D Seminar*, 2007.

[5] Lennert Bentrup and Hoffman M., "Free Routing Airspace in Europe," *International Conference on Research in Air Transportation*, 2016.

[6] AirTOpsoft S. A., http://airtopsoft.com/en-route-simulation, 2018.

[7] Eurocontrol, *User Manual for tha Base of Aircraft DAta (BADA) Revision 3.8*, 2010.

[8] Nakamura Y. and Kageyama K., "A Study on Free Routing Considering Interference of Air Traffic Flow," *Modeling and Simulation Technology Conference, SciTech*, 2017.

[9] Pierre Flener, Pearson J., "Automatic Airspace Sectorisation: A Survey," 2013.

Contact Author Email Address

mailto: kage@mpat.go.jp

Copyright Statement